substance: boron compounds with lanthanides
property: properties of lanthanide hexaborides: LaB_6

Structure, chemical bond

cP7-CaB_6 type structure

Structure in Fig. 1.

Space group: $Pm\bar{3}m$

Growth and crystal data for preparation by high temperature solution growth [84L] and references therein.

X-ray diffraction (compared with CaB_6, YbB_6 and ThB_6) [82B].

Preparation by pressureless sintering [87K3].

Neutron and X-ray diffraction of the crystal structure of rare earth hexaborides [87K1].

Investigation of different steps of structural perfection of monocrystalline LaB_6 [89K1].

X-ray structural investigation of single crystals of lanthanum, cerium and samarium hexaborides [86E].

Thermal analysis of float-zone traveling solvent crystal growth of LaB_6 [96L2].

Preparation of LaB_6 single crystals from a boron-rich molten zone by the floating zone method [93O1, 93O2].

Preparation of LaB_6 and (La, Ce)B_6 single crystals by the traveling solvent floating zone method in [94O1].

Preparation of LaB_6 single crystals by the traveling solvent floating zone method, dependence of the boundary density on the La weight used in [92O3].

A thermodynamic analysis of lanthanum hexaboride crystal preparation from aluminum flux with the use of compound precursors [97P].

Automatic preparation of LaB_6 single crystals by the floating zone technique [90O].

Directional crystallization during eutectic growth of LaB_6 single crystals in ZrB_2 [91P1, 94P1]; see also [85E].

A critical review of available data shows that the homogeneity range of LaB_6 is narrow with a variation in the B/La ratio of less than 2 % up to 2000 K. Above that temperature it widens appreciably [86L].

The incorporation of convection in 1D models of float zone and traveling solvent techniques applied to LaB_6 [96L1].

An atom-probe analysis of the LaB_6(001) plane [83M].

Real structure of LaB_6 single crystals [87P].

Cluster formation at LaB_6 field evaporation: theory and experiment [99B].

lattice parameters
(in Å)

a	4.1569(1)	T = 300 K	(LaB_6, T_{prep} = 1700 K)	84K
	4.1566(1)		(LaB_5, T_{prep} = 1400 K)	
	4.1571		(LaB_9, T_{prep} = 2100 K)	
	4.1563	T = 300 K	La-rich, La defect 0 %	93O2
	4.1566		nearly stoichiometric, La defect 0 %	
	4.1564		B-rich, La defect 0.1 %	
	4.1563		B-rich, La defect 1.1%	

lattice parameters in homogeneity range

a	4.1563(1)	*T* = 304(1) K	LaB_6, X-ray diffraction,	83P
	4.1565(1)		$La_{0.94}B_6$	
	4.1561(2)		$La_{0.9}B_6$	
	4.1562(2)		$La_{0.81}B_6$	
	4.1567(2)		$La_{0.75}B_6$	

interatomic distances for LaB_6
(in Å)

d	3.054(1)	*T* = 300 K	La – 24B	84K
	1.659(1)		B – 1B	
	1.766(1)		B – 4B	
	2.498(1)		B – 1B	
	3.054(1)		B – 4La	

X-ray diffractometry in [84K].

Structure refinement (boron site occupancy 96.4...98.2 %) in [84K, 86K1].

Atomic structure of the LaB_6 (100) surface as observed with scanning tunneling microscopy [92O4].

For lattice parameters see also [90B].

NMR studies of borates and borides in [86B4].

Review on the homogeneous range and various properties concerning application, in particular influence of oxygen water vapor, methane gas, hydrogen gas on the cathode emission in [94P1].

Ternary phase equilibria of the La-Cu-B system at 650°C [90B].

Electronic properties

Calculation of the electronic band structure (FLAPW method) and positron annihilation in LaB_6 (compared with CeB_6) [89K2].

Electronic band structure in Fig. 2 [89K2].

energy gap

E_g	~ 2 eV	*T* = 300 K	optical absorption	80G

Optical absorption spectrum in the range of the absorption edge in Fig. 3 [80G].

B K emission and absorption spectrum (compared with SmB_6 and EuB_6) [82O].

X-ray absorption spectra in [75P2].

average inner lattice potential

Φ	9.78 eV	experiment	86K2
	9.76 eV	theory	

average work function of electrons
(in eV)

ϕ_e	2.81		experiment	86K2
	2.82		theory	
	2.73	T = 1200...1400 K	(100) pure LaB_6	92O1
	3.53	T = 1200...1400 K	(100) $La_{0.7}Ce_{0.3}B_6$	
	3.44	T = 1200...1400 K	(100) $La_{0.82}Pr_{0.18}B_6$	
	2.70	T = 1200...1400 K	(100) $La_{0.85}Nd_{0.15}B_6$	
	2.51	T = 1200...1400 K	(110) $La_{0.82}Pr_{0.18}B_6$	
	2.4	T = 300 K	(100) $LaB_{6.0}$	96O2
	2.4	T = 300 K	(100) $LaB_{6.14}$	

Work function of the LaB_6 (100) surface in Fig. 4 [79S, 81M, 86B1].

The emission characteristics remained unchanged for 864 h in a SEM (scanning electron microscope); evaporation loss 0.07 μm h^{-1} [92O1].

Richardson plot of pure LaB_6 and LaB_6 with Ce, Pr, Nd partly substituted for La in Fig. 5 and brightness plot in Fig. 6 [92O1].

Richardson plot for LaB_6 (and CeB_6) with excess B ($LaB_{6.06}$ and $CeB_{6.07}$) compared with pure crystals in Fig. 7 [96O1].

Thermionic emission properties of LaB_6 (compared with CeB_6) in [96O1, 96O2]

Thermionic emission and vaporization behavior of ternary systems based on LaB_6 [83S].

Calculated electron density distribution in Fig. 8 [75P1, 81S].

Calculated electron density distributions also in [82S] and [86B2].

possible transition energies for LaB_6
(for the definition of the transitions cp. Fig. 8)

Transition	Transition energy E [eV]		
	calc.	obs.	
A-E_F	4.3	2.4	81S
		3.6	
A-b	5.3	5.5	
	calc.	obs.	
A-c	7.3	7.1	
B-b, A'-c	9.1;9.0	9.4	
C-b	11.4	11.6	
D-b	14.7	15.0	
E-c	25.2	25.0	

Auger-type electron emission from energetic He^+ ions interacting with the LaB_6 (100) surface in Fig. 9 [96S].

critical temperature of superconductivity

T_c	0.122 K	91F, 75A

Impurities and defects

Preparation of Nd-substituted LaB_6 single crystals by the floating zone method, dependence of boundary density on Nd content in [92O2].

Variation of the lattice constants in Ce, Pr and Nd substituted LaB_6 in Fig. 10 [92O2].

The system of solid solutions $Sm_xLa_{1-x}B_6$ [79A].

ESR study of $EuB_{6-x}C_x$ including the comparison with some corresponding $YbB_{6-x}C_x$, $SrB_{6-x}C_x$, $Eu_{1-x}Gd_xB_6$, $Eu_{1-x}Sr_xB_6$ and $Eu_{1-x}La_xB_6$ compounds in [81T].

Irradiation-induced damage rates in [95C].

Spectroscopic investigation of lattice vacancies in [93Y] ; Raman spectra of samples with excess B in Fig. 11; comparison of observed Raman wavenumbers with calculated dispersion curves in Fig. 12 [93Y].

Thermal vibration of atoms in several metal hexaborides in [73D1].

Some pecularities of the eutectic crystallization of LaB_6 – (Ti, Zr)B_2 alloys [99P].

Lattice properties

Force constants [90Y, 93N].

For vibrational frequencies [88T, 90Y, 93Y].

phonon modes

(in meV)

T_{1u} (acoustic)	12.85(10)	T = 1.7...4.2 K	PC spectrum *)	
			neutron spectrum	91S1
T_{1g}	25.68(7)	T = 300 K	Raman	
	24.00(6)	T = 1.7...4.2 K	PC and neutron	
T_{1u} (trans. opt.)	37.17(20)	T = 1.7...4.2 K	PC and neutron	
T_{1u} (long. opt.)	51.89(26)	T = 1.7...4.2 K	PC and neutron	
T_{2u}	69.62(19)	T = 1.7...4.2 K	PC and neutron	
T_{2g}	84.20(12)	T = 300 K	Raman	
	84.29(42)	T = 1.7...4.2 K	PC and neutron	
T_{1u}	104.2(4)	T = 1.7...4.2 K	PC and neutron	
E_g	139.6(1)	T = 300 K	Raman	
	140.3(3)	T = 1.7...4.2 K	PC and neutron	
A_{1g}	155.5(2)	T = 300 K	Raman	
	155.6(10)	T = 1.7...4.2 K	PC and neutron	

*) PC = point contact

phonon resonance wavenumbers

(in cm^{-1})

ν/c	85	T = 300 K	from FT-Raman spectroscopy	97S
	104			
	203			
	291			
	499			
	573			
	683			
	730			
	787			
	1105			
	1195			

elastic constants

(in 10^{11} dyn cm^{-2})

c_{11}	45.33	calculated (one specific model)	85T
	45.33(11)	experimental	
c_{12}	1.82	calculated	77T
	1.82(17)	experimental	
c_{44}	9.52	calculated	85S

	9.01(5)		experimental	
sound velocity (in m s^{-1})				
v_s	9793	T = 300 K	longitudinal, [001]	77T
	4362		transverse, [001], polarization [$1\bar{1}0$]	
	4335		transverse, [110], polarization [001]	
	6830		transverse, [110], polarization [$1\bar{1}0$]	
	7779		longitudinal, [111]	
r.m.s. velocity (in m s^{-1})				
v	9810	(T = 300 K)	longitudinal, [001]	77T
	4374		transverse, [001], polarization [$1\bar{1}0$]	
	6796		transverse, [110], polarization [$1\bar{1}0$]	
	7756		longitudinal, [111]	

For a comparison of the phonon modes of LaB_6 with those of other metal hexaborides, see Figs. 13 and 14.

Theoretical study of lattice dynamics; calculated phonon dispersion curves in Fig. 15 [85T].

Point contact spectra of the electron-phonon interaction in Fig. 16 [88S].

Phonon dispersion curves of $La^{11}B_6$ measured by inelastic neutron scattering in Fig. 17 [85S].

Comparison of the phonon spectrum of LaB_6, experimental and theoretical results: FT Raman spectrum [97S]; point contact spectrum [88S]; density of states determined by inelastic neutron scattering [82S], theoretically calculated densities of states [78G, 82S]. All in Fig. 18.

Low frequency part of the FT-Raman spectrum [97S] compared with the phonon branches obtained on $La^{11}B_6$ by inelastic neutron scattering [85S] in Fig. 19.

High resolution electron loss spectroscopy to determine vibrational spectra of pure surfaces and of surface covered with oxygen [93N, 96R2, 96R1, 96Y1, 96Y2]; typical spectra in Fig. 20.

Theoretical phonon dispersion curves of LaB_6 compared with SmB_6 (see there) in [91A].

Lattice dynamics of LaB_6 between 35 and 500 K studied by 0.9 MeV ion channeling: La in the Einstein model [86P].

Theoretical study of lattice dynamics; theoretical phonon dispersion curves in [85T] and in [82S].

IR diffuse reflection and Raman spectra (La, Nd, Gd, Tb, Dy, Yb)B_6 in Fig. 21 [88T, 93Y].

Raman spectra and frequencies see also document **properties of lanthanide hexaborides: YbB_6** (optical properties)

Thermal expansion coefficient: α [$10^{-6}K^{-1}$] = 4.1547 (1+5.48·10^{-6} T + 1.79·10^{-9} T^2), T in K [73D1].

Transport properties

Electrical properties of several hexaborides in [69P].

Electrical properties of some rare earth hexaborides in [62S].

The Eliashberg function and the superconducing T_c [80S].

resistivity
(in Ω cm)

ρ	$1.3 \cdot 10^{-5}$	T = 300 K		91S1
	$1.1 \cdot 10^{-5}$	T = 4.2 K	La-rich	93O2
	0.04		nearly stoichiometric	
	0.17		B-rich, La defect 0.1 %	
	0.53		B-rich La defect 1.1 %	
	$1.5 \cdot 10^{-5}$ Ω cm	T = 300 K		80L

thermoelectric power

S	~0.9 μV K^{-1}	T = 300 K	p = 0.1 MPa	91S1
	~1.8 μV K^{-1}	T = 300 K	p = 11 GPa	

Pressure dependence of the electrical resistivity; ρ(p)/ρ(0) vs. hydrostatic pressure p (compared with SmB_6, YbB_6 and EuB_6) in Fig. 22 [81K, 91S1].

Pressure dependence of the thermoelectric power compared with LaB_6 and YbB_6 in Fig. 23 [91S1].

Electrical properties in [91P2].

Optical properties

Dielectric function up to 42 eV in Fig. 24 [81S, 80G].

reflectivity minimum
(E in eV)

R_{min}	0.01	T = 300 K		81S
E (R_{min})	2.1			
E (R_{min})	2.111	T = 300 K	single crystal after annealing	94K
	2.111		powder	
	1.92	T = 300 K	film deposited at 200 °C	80B
	2.11(1)		film deposited at 550 °C	
	2.17(1)		film deposited at 650 °C	
	2.05(1)		molten	

Optical reflectivity spectra of LaB_6 (molten and deposited films) in Fig. 25 [80B].

Reflectivity spectrum in Fig. 26 [81S, 80G]. See also document **properties of lanthanide hexaborides: YbB_6**

Influence of mechanical polishing on the reflectivity spectra in [94K].

Absorption spectrum in [80G].

Raman spectra of LaB_6 synthesized with an excess of boron in Fig. 11 [93Y].

Comparison of observed Raman wavenumbers and calculated dispersion curve in Fig. 12 [93Y].

Raman spectrum of amorphous LaB_6 in [80L].

Differences between LaB_6 and CeB_6 by means of spectroscopic ellipsometry [86V].

Further properties

compressibility

κ	$0.58(3) \cdot 10^{-11}$ Pa^{-1}	T = 300 K	X-ray power diffraction	82L
	$0.61 \cdot 10^{-11}$ Pa^{-1}		calculated from elastic constants	

entropy

S	83.16(21) J mol^{-1}K^{-1}		86B2

Entropy of LaB_6 depending on temperature in Fig. 27 [80F].

melting point

T_m	2715 °C	96G

Temperature dependence of C_p and C_p/T^3 in Fig. 28 [91P2, 91S1, 85P, 78R].

Detailed discussion of thermal properties in [91P2, 91S1].

microhardness
(in kg mm^{-2})

H_V	~1500	T = 300 K		93O3
H_K	2250	T = 300 K,	cube, average value; load 20 g	96G
	2160		cube, average value; load 50 g	
	2040		cube, average value; load 100 g	
	1900		cube, average value; load 200 g	
	1800		rhombododecahedron, average value., load 50 g	

Temperature dependence of the hardness of pure and partly Ce substituted LaB_6 in Fig. 29 [94O1].

Temperature dependence of Vickers microhardness in [93O1, 90G].

Anisotropy of Vickers microhardness depending on T [93O1].

Dependence of measured Vickers hardness on the penetration depth [90G].

High temperature hardness of single crystals of LaB_6, CeB_6, PrB_6, NdB_6 and SmB_6 [99O].

On LaB_6 as a thermionic cathode material [94Y].

Search for rugged, efficient photocathode materials (LaB_6 and CeB_6) [92B].

Desorption of the LaB_6 (100) surface in [94O2].

Surface states on the LaB_6 (100), (110) and (111) clean surfaces studied by angle-resolved UPS [80N].

Evaporation rates from (100) planes of LaB_6 (compared with $LaB_{6.06}$, CeB_6, and $CeB_{6.07}$ in Fig. 30 [96O1].

Oxygen adsorption sites on the LaB_6 (100) (compared with PrB_6 (100)) surfaces [96Y1].

Oxygen adsorption on LaB_6 (100) and (111) surfaces [96Y2].

Reaction of LaB_6 with water and oxygen; IR absorption spectra of oxidized LaB_6 [87G1].

Debye temperature
(in K)

Θ_D	885	T = 0...1073 K	X-ray, thermal expansion	61Z
	720	0...973 K	X-ray, powder	73D2
	491	300 K	X-ray, single crystal	87K1
	732		boron sublattice	
	417		metal sublattice	
	773	300 K	elastic constant	76T
	468	low T	electrical resistance	76T
	245	300 K	electrical resistance	77T
	404	300K	ultrasonic method	77T
	773	300K	ultrasonic method	85S
	212	0...10 K	specific heat	70E
	250	0...10 K	specific heat	69M

For a detailed discussion on the role of interatomic interactions in the characteristic Debye temperature of rare earth hexaborides, see [91S1]. For Einstein temperatures of metal hexaborides see Fig. 31.

References:

61Z Zhuravlev, N.N., Stepanova, A.A., Paderno, Yu.B., Samsonov, G.V.: Sov. Phys. Crystallogr. 6 (1961) 636.

62S Samsonov, G.V., Paderno, Yu.B.: in: Vsokotemperaturnaye metallokeramicheskie materialne, AN USSR: Kiev, 1962, p. 102 (in Russian).

69M Mercurio, J.P., Etourneau, J., Naslain, R., Hagenmuller, P.: C. R. Acad. Sci. (Paris) B 268 (1969) 1766.

69P Paderno, Yu.B., Novikov, V.I., Garf, E.S.: Poroshk. Metall. 11 (1969) 70 (in Russian).

70E Etourneau, J., Mercurio, J.P., Naslain, R., Hagenmuller, P.: J. Solid State Chem. 2 (1970) 332.

73D1 Dudchak, Ya.I., Fedishin, Ya.I., Paderno, Yu.B., Vadez, D.I.: Izv. Akad. Nauk. SSSR Ser. Fiz. 1 (1973) 154 (in Russian).

73D2 Dutchak, Ya.I., Fedishin, Ya.I., Paderno, Yu.B., Vadets, D.I.: Izv. V.U.Z. Fiz. (1973) 154.

75A Arko, A.J., Crabtree, G.W., Karim, D., Ketterson, J.B., Mueller, F.M., Walch, P.F., Windmiller, L.R., Fisk, Z., Hoyt, R.F.: Int. J. Quantum Chem. Symp. 9 (1975) 569.

75P1 Perkins, P.G., Armstrong, D.R., Breeze, A.: J. Phys. C 8 (1975) 3558.

75P2 Paderno, Yu.B., Ivanchenko, L.A., Bessaraba, V.I., Beretchak, V.M.: Poroshk. Metall. 6 (1975) 106 (in Russian).

76T Tanaka, T., Akahane, T., Bannai, E.: J. Phys. C 9 (1976) 1235.

77T Tanaka, T., Yoshimoto, J., Ishii, M.: Solid State Commun. 22 (1977) 203.

78G Gompf, F.: in: Prog. Report Teilinstitut Nukleare Festkörperphysik KfK 2670, K. Käfer ed., Kernforschungszentrum Karlsruhe: Karlsruhe, 1978, p. 17.

78R Report Nat. Inst. Research in Inorg. Mater. 17 (1978) 44.

79A Aivasov, M.I., Aleksandrovich, S.V., Evseev, B.A., Zinchenko, K.A., Mkrtchyan, V.S.: Inorg. Mater. 15 (1979) 48.

79S Swanson, L.W., Mc Neely, D.R.: Surf. Sci. 83 (1979) 11.

80B Bessaraba, V.I., Makarenko, T.I., Paderno, Yu.B.: Journal Prikladnoi Spectroscopii 33 (1980) 527 (in Russian).

80F Fujita, T., Suzuki, M., Isikawa, Y.: Solid State Commun. 33 (1980) 947.

80G Gurin, V.N., Korsukova, M.M., Karin, M.G., Sidorin, K.K., Smirnov, I.A., Shelikh, A.I.: Sov. Phys. Solid State 22 (1980) 418.

80L Lannin, J.S., Messier, R.: Phys. Rev. Lett. 45 (1980) 1119.

80N Nishitani, R., Aono, M., Tanaka, T., Kawai, S., Iwasaki, H., Oshima, C., Nakamura, S.: Surf. Sci. 95 (1980) 341.

80S Schell, G., Winter, H., Rietschel, H.: in: Superconductivity in d- and f-band metals. Proc. Conf. Supercond. In d- and f-band metals, H. Suhl, M.B. Maple ed., Academic: London, 1980, p. 465.

81K Korsukova, M.M., Stepanov, N.N., Gontcharova, E.V., Gurin, V.N., Nikanorov, S.P., Smirnov, I.A.: J. Less-Common Met. 82 (1981) 211. (Proc. 7th Int. Symp. Boron, Borides and Rel. Compounds, Uppsala, Sweden, 1981).

81M Morosov, V.V., Loboda, P.I., Siman, N.I.: in: Proc. Konf. po emissionnoy elektronike, NAUKA: Moscow, 1981, p. 183 (in Russian).

81S Shelykh, A.I., Sidorin, K.K., Karin, M.G., Bobrikov, V.N., Korsukova, M.M., Gurin, V.N., Smirnov, I.A.: J. Less-Common Met. 82 (1981) 291.

81T Tarascon, J.M., Etourneau, J., Dance, J.M., Hagenmuller, P., Georges, R., Angelov, S., v. Molnar, S.: J. Less-Common Met. 82 (1981) 277 (Proc. 7th Int. Symp. Boron, Borides and Rel. Compounds, Uppsala, Sweden, 1981).

82B Barantseva, I.G., Paderno, Yu.B.: Sov. Powder Metall. Met. Ceram. 21 (1982) 585.

82L Lundström, T., Lönnberg, B., Törmä, B.: Phys. Scr. 26 (1982) 414.

82O Okusawa, M., Ichikawa, K., Matsumoto, T., Tsutsumi, K.: J. Phys. Soc. Jpn. 51 (1982) 1921.

82S Schell, G., Winter, H., Rietschel, H., Gompf, F.: Phys. Rev. B 25 (1982) 1589.

83M Murakami, K., Adachi, T., Uroda, T., Nakamura, S., Komoda, O.: Surf. Sci. 124 (1983) L25.

83P Paderno, Yu.B., Lundström, T.: Acta Chem. Scand. A 37 (1983) 609.

83S Storms, E.K.: J. Appl. Phys. 54 (1983) 1076.

84K Korsukova, M.M., Lundström, T., Gurin, V.N., Tergenius, L.-E.: Z. Kristallogr. 168 (1984) 299.

84L Lundström, T.: J. Less-Common Met. 100 (1984) 215.

85E Echigoya, J., Suto, H., Hayashi, S.: Trans. Jap. Inst. Met. 26 (1985) 895.

85P Peysson, Y., Ayache, C., Sales, B.: J. Magn. Magn. Mater. 47 & 48 (1985) 63.

85S Smith, H.G., Dolling, G., Kunii, S., Kasaya, M., Liu, B., Takegahara, K., Kasuya, T., Goto, T.: Solid State Commun. 53 (1985) 15.

85T Takegahara, K., Kasuya, : Solid State Commun. 53 (1985) 21.

86B1 Bul'ga, A.V., Kapustin, N.F., Solonovich, V.K., Paderno, Yu.B., Kovalev, A:V.: Electron. Tekh. 2(213) (1986) 13 (in Russian).
86B2 Bullett, D.W.: in: Boron-Rich Solids (AIP Conf. Proc. 140), Albuquerque, New Mexico 1985, D. Emin, T.L. Aselage, C.L. Beckel, I.A. Howard ed., American Institute of Physics: New York, 1986, p. 249.
86B3 Borovikova, M.S., Fesenko, V.V.: J. Less-Common Met. 117 (1986) 287. (Proc. 8th Int. Symp. Boron, Borides, Carbides, Nitrides and Rel. Compounds, Tbilisi, Oct. 8 - 12, 1984)
86B4 Bray, P.J.: in: Boron-Rich Solids (AIP Conf. Proc. 140), Albuquerque, New Mexico 1985, D. Emin, T.L. Aselage, C.L. Beckel, I.A. Howard ed., American Institute of Physics: New York, 1986, p. 142.
86E Eliseev, A.A., Efremov, V.A., Kuz'micheva, G.M., Konovalova, E.S., Lazorenko, V.I., Paderno, Yu.B., Khlustova, S.Yu., Yu, S.: Sov. Phys. Crystallogr. 31 (1986) 476.
86K1 Korsukova, M.M., Gurin, V.N., Lundström, T., Tergenius, L.-E.: J. Less-Common Met. 117 (1986) 73 (Proc. 8th Int. Symp. Boron, Borides, Carbides, Nitrides and Rel. Compounds, Tbilisi, Oct. 8 - 12, 1984).
86K2 Kutelia, E.R., Dzimtseshvili, O.G., Dzigrashvili, T.A., Tsivsivadze, D.M., Kervalishvili, P.D.: J. Less-Common Met. 117 (1986) 283 (Proc. 8th Int. Symp. Boron, Borides, Carbides, Nitrides and Rel. Compounds, Tbilisi, Oct. 8 - 12, 1984).
86L Lundström, T.: Z. Anorg. Allg. Chem. 540/541 (1986) 163.
86P Peysson, Y., Daudin, B., Dubus, M., Berenson, R.E.: Phys. Rev. B 34 (1986) 8367.
86V van der Heide, P.A.M., ten Cate, H.W., ten Dam, L.M., der Groot, R.A., de Vroomen, A.R.: J. Phys. F: Met. Phys. 16 (1986) 1617.
86Z Zirngiebl, E., Blumenröder, S., Mock, R., Güntherodt, G.: J. Magn. Magn. Mater. 54-57 (1986) 359.
87G1 Gerlach, U., Krabbes, G., Krausse, R., Stöver, G.: in: Proc. 9th Int. Symp. Boron, Borides and Rel. Compounds, University of Duisburg, Germany, Sept. 21 - 25, 1987, H. Werheit ed., University of Duisburg: Duisburg, Germany, 1987, p. 311.
87G2 Gurin, V.N., Korsukova, M.M., Kuz'ma, Yu.B., Chaban, N.F., Nechitailov, A.A., Haupt, H., Werheit, H.: in: Proc. 9th Int. Symp. Boron, Borides and Rel. Compounds, University of Duisburg, Germany, Sept. 21 - 25, 1987, H. Werheit ed., University of Duisburg: Duisburg, 1987, p. 275.
87K1 Korsukova, M.M., Gurin, V.N., Nikanorov, S.P., Trunov, V.A., Kudryashev, V.A., Ulyanov, V.A., Antson, O., Hiismäki, P., Mutka, H., Pcyry, H, Tiitta, A.: in: Preprint 1188, Akad. Nauk SSSR, Fiz. Tekh. Inst. im., A.F. Ioffe, ed., Leningrad, 1987
87K2 Ku, H.C., Tai, M.F., Klavins, P., Shelton, R.N.: Jpn. J. Appl. Phys. Suppl. 26 (1987) 827.
87K3 Knoch, H., Lipp, A.: in: Novel Refractory Semiconductors, MRS Symp. Proc. Vol. 97, D. Emin, T.L. Aselage, C. Wood ed., Materials Research Soc.: Pittsburgh, 1987, p. 119.
87P Pilyankevich, A.N., Britun, V.F.: in: Proc. 9th Int. Symp. Boron, Borides and Rel. Compounds, University of Duisburg, Germany, Sept. 21 - 25, 1987, H. Werheit ed., University of Duisburg: Duisburg, 1987, p. 270.
88S Samuely, P., Reiffers, M., Flachbart, K., Akimenko, A.I., Janson, J.K., Ponomarenko, N.M., Paderno, Yu.B.: J. Low Temp. Phys. 71 (1988) 49.
88T Turrell, S., Yahia, Z., Huvenne, J.P., Lacroix, B., Turrell, G.: J. Mol. Struct. 174 (1988) 455.
89K1 Kovalev, A.V., Tkachenko, V.F., Taran, A.A., Paderno, Yu.B., Paderno, V.N.: Neorg. Mater. 25 (1989) 968.
89K2 Kubo, Y., Asano, S.: Phys. Rev . B 39 (1989) 8822.
90B Bolmgren, H., Lundström, T.: J. Less-Common Met. 163 (1990) 79.
90G Gridneva, I.B., Lazorenko, V.I., Lozko, D.V., Mil'man, Yu.B., Paderno, Yu.B., Tshugunova, S.I.: Poroshk. Metall. 12 (1990) 30.
90O Otani, S.., Tanaka, T., Ishizawa, Y.: J. Cryst. Growth 100 (1990) 658.
90Y Yahia, Z., Turrell, S., Turrell, G., Mercurio, J.P.: J. Mol. Struct. 224 (1990) 303.
91A Alekseev, P.A., Ivanov, A.S., Kikoin, K.A., Mischenko, A.S., Lazukov, A.N., Rumyantsev, A.Yu., Sadikov, I.P., Konovalova, E.S., Paderno, Yu.B.: in: Boron-Rich Solids, Proc. 10th Int. Symp. Boron, Borides and Rel. Compounds, Albuquerque, NM 1990 (AIP Conf. Proc. 231), D. Emin, T.L. Aselage, A.C. Switendick, B. Morosin, C.L. Beckel ed., American Institute of Physics: New York, 1991, p. 318.
91F Fisk, Z.: in: Boron-Rich Solids, Proc. 10th Int. Symp. Boron, Borides and Rel. Compounds, Albuquerque, NM 1990 (AIP Conf. Proc. 231), D. Emin, T.L. Aselage, A.C. Switendick, B. Morosin, C.L. Beckel ed., American Institute of Physics: New York, 1991, p. 155.
91P1 Paderno, Yu.B., Paderno, V.N., Filippov, V.: in: Boron-Rich Solids (AIP Conf. Proc. 231), Albuquerque, New Mexico 1990, D. Emin, T. Aselage, A.C. Switendick, B. Morosin and C.L. Beckel ed., American Institute of Physics: New York, 1991, p. 561.
91P2 Paderno, Yu.B., Shizevalova, N.Yu., Muratov, V.B.: in: Boridi, Akad. NAUK Ukrainian SSR, Institue for problems of materials science ed., Kiev, 1991 (in Russian).

91S1 Sidorov, V.A., Stepanov, N.N., Ziok, O.B., Chvostanzev, L.G., Smirnov, N.A., Korsukova, M.M.: Fiz. Tverd. Tela 33 (1991) 1271(in Russian).

91S2 Shitsevalova, N.Yu., Paderno, Yu.B.: in: Boron-Rich Solids, Proc. 10th Int. Symp. Boron, Borides and Rel. Compounds, Albuquerque, NM 1990 (AIP Conf. Proc. 231), D. Emin, T.L. Aselage, A.C. Switendick, B. Morosin, C.L. Beckel ed., American Institute of Physics: New York, 1991, p. 326.

92B Bamford, D.J., Bakshi, M.H., Deacon, D.A.G.: Nucl. Instrum. Methods A 318 (1992) 377.

92O1 Otani, S., Hiraoka, H., Ide, M., Ishizawa, Y.: J. Alloys Compounds 189 (1992) L1.

92O2 Otani, S., Honma, S., Tanaka, T., Ishizawa, Y.: J. Alloys Compounds 179 (1992) 201.

92O3 Otani, S., Ishizawa, Y.: J. Cryst. Growth 118 (1992) 461.

92O4 Ozcomert, J.S., Trenary, M.: J. Vac. Sci. Technol. A 10 (1992) 684.

93N Nagao, T., Kitamura, K., Iizuka, Y., Oshima, C., Otani, S.: Surf. Sci. 290 (1993) 436.

93O1 Otani, S., Honma, S., Ishizawa, Y.: J. Alloys Compounds 193 (1993) 286.

93O2 Otani, S., Honma, S., Yajima, Y., Ishizawa, Y.: J. Cryst. Growth 126 (1993) 466.

93O3 Otani, S., Tanaka, T., Ishizawa, Y.: J. Alloys Compounds 202 (1993) L25.

93Y Yahia, Z., Turrel, S., Mercurio, J.P., Turrel, G.: J. Raman Spectroscopy 24 (1993) 207.

94K Konovalova, E., Paderno, Yu.B., Khoynenko, N.: Proc. 11th Int. Symp. Boron, Borides and Rel. Compounds, Tsukuba, Japan, August 22 - 26, 1993, Jpn. J. Appl. Phys. Series 10 (1994), p. 126.

94O1 Otani, S., Honma, S., Tanaka, T., Ishizawa, Y.: Proc. 11th Int. Symp. Boron, Borides and Rel. Compounds, Tsukuba, Japan, August 22 - 26, 1993, Jpn. J. Appl. Phys. Series 10 (1994), p. 114.

94O2 Ozcomert, J.S., Trenary, M.: Proc. 11th Int. Symp. Boron, Borides and Rel. Compounds, Tsukuba, Japan, August 22 - 26, 1993, Jpn. J. Appl. Phys. Series 10 (1994), p. 174.

94P1 Paderno, Y., Paderno, V., Filippov, V.: Proc. 11th Int. Symp. Boron, Borides and Rel. Compounds, Tsukuba, Japan, August 22 - 26, 1993, Jpn. J. Appl. Phys. Series 10 (1994), p. 190.

94P2 Peshev, P.: Proc. 11th Int. Symp. Boron, Borides and Rel. Compounds, Tsukuba, Japan, August 22 - 26, 1993, Jpn. J. Appl. Phys. Series 10 (1994), p. 118.

94Y Yang, P., Aselage, T.L.: Proc. 11th Int. Symp. Boron, Borides and Rel. Compounds, Tsukuba, Japan, August 22 - 26, 1993, Jpn. J. Appl. Phys. Series 10 (1994), p. 130.

95C Carrard, M., Emin, D., Zuppiroli, L.: Phys. Rev. B 51 (1995) 11270.

96G Gurin, V.N., Derkachenko, L.I., Korsukova, M.M., Nikanorov, S.P., Jung, W., Müller, R.: Sov. Phys. Solid State 38 (1996) 1508.

96L1 Louchev, O., Otani, S., Ishizawa, Y.: J. Cryst. Growth 167 (1996) 333.

96L2 Louchev, O., Otani, S., Ishizawa, Y.: J. Appl. Phys. 80 (1996) 518.

96O1 Otani, S., Ishizawa, Y.: J. Alloys Compounds 245 (1996) L18.

96O2 Otani, S., Souda, R., Ishizawa, Y.: J. Ceram Soc. Jpn. Inter. Ed. 104 (1996) 1088.

96R1 Rokuta, E., Yamamoto, N., Hasewaga, Y., Nagao, T., Trenary, M., Oshima, C., Otani, S.: Surf. Sci. 357/358 (1996) 712.

96R2 Rokuta, E., Yamamoto, N., Hasegawa, Y., Nagao, T., Trenary, M., Oshima, C., Otani, S.: J. Vac. Sci. Technol. A 14 (1996) 1674.

96S Souda, R., Hayami, W., Aizawa, T., Otani, S., Ishizawa, Y.: Surf. Sci. 363 (1996) 133.

96Y1 Yamamoto, N., Rokuta, E., Hasegawa, Y., Nagao, T., Trenary, M., Oshima, C., Otani, S.: Surf. Sci. 348 (1996) 133.

96Y2 Yamamoto, N., Rokuta, E., Hasegawa, Y., Nagao, T., Trenary, M., Oshima, C., Otani, S.: Surf. Sci. 357/358 (1996) 708.

97P Peshev, P.: J. Solid State Chem. 133 (1997) 237 (Proc. 12th Int. Symp. Boron, Borides and Rel. Compounds, Baden, Austria, 1996).

97S Schmechel, R., Werheit, H., Paderno, Yu.B.: J. Solid State Chem. 133 (1997) 264 (Proc. 12th Int. Symp. Boron, Borides and Rel. Compounds, Baden, Austria, 1996).

99B Buenker, R., Boustani, I., Hirsch, G., Gurin, V.N., Korsukova, M.M., Loginov, M.V., Shrednik, V.N.: J. Solid State Chem. (2000) (Proc. 13th Int. Symp. Boron, Borides and Rel. Compounds, Dinard, France, Sept. 1999).

99O Otani, S., Nakagawa, H., Nishi, Y., Kieda, N.: J. Solid State Chem. (2000) (Proc. 13th Int. Symp. Boron, Borides and Rel. Compounds, Dinard, France, Sept. 1999).

99P Paderno, Yu.B., Paderno, V.N., Filippov, V.: J. Solid State Chem. (2000) (Proc. 13th Int. Symp. Boron, Borides and Rel. Compounds, Dinard, France, Sept. 1999).

99T Takahashi, Y., Ohshima, K., Okamura, F.P., Otani, S., Tanaka, T.: J. Phys. Soc. Jpn. 68 (1999) 2304.

99W Werheit, H., Au, T., Schmechel, R., Paderno, Yu.B., Konovalova, E.S.: J. Solid State Chem. (2000) (Proc. 13th Int. Symp. Boron, Borides and Rel. Compounds, Dinard, France, Sept. 1999).

Fig. 1.

Metal hexaborides. Unit cell with B_6 octahedra at the corners and the metal (M) atom in the center.

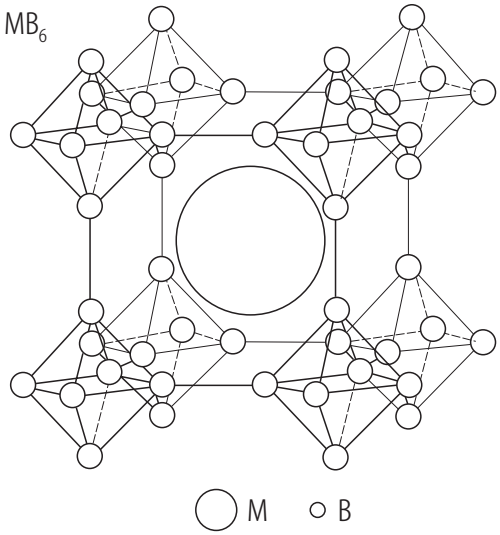

Fig. 2.

LaB_6. Calculated energy-band structure; dashed line: Fermi level [89K2].

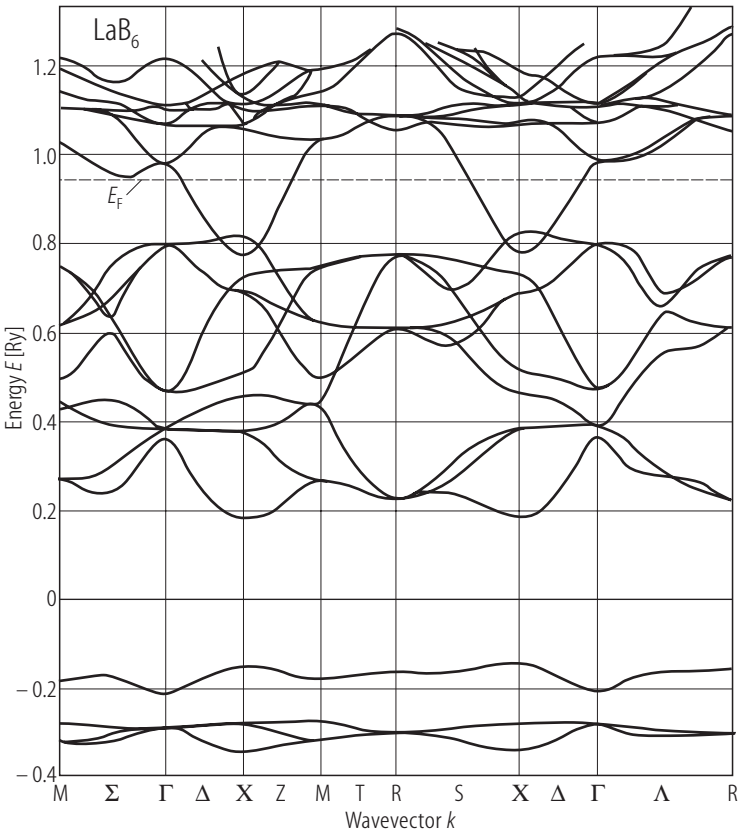

Fig. 3

LaB_6. Absorption coefficient α vs. photon energy. Insert: Plot in relative units according to direct forbidden interband transitions [80G].

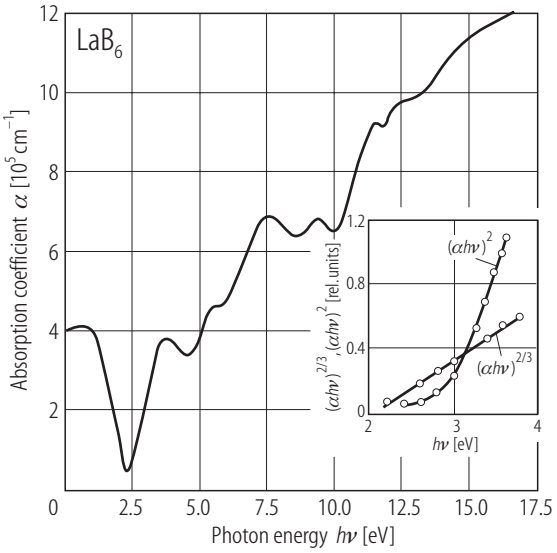

Fig. 4

LaB_6. Work function of the LaB_6 (100) surface. (*1*) [86B10], (*2*) [81M], (*3*) [79S].

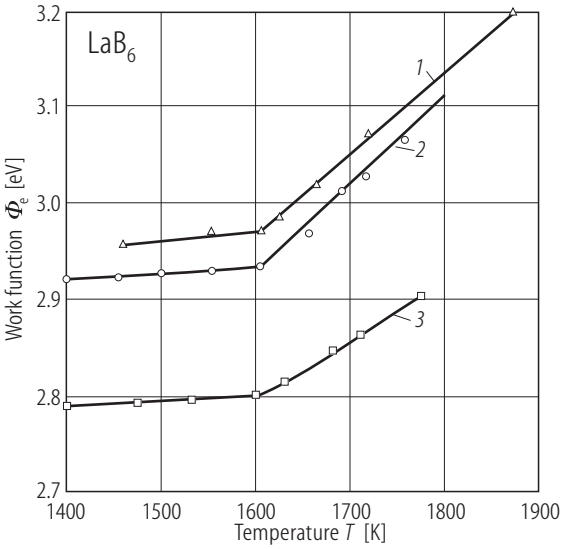

Fig. 5

LaB_6 (:Ce, Pr, Nd). Richardson plots for pure LaB_6(100), and LaB_6 with Ce, Nd and Pr substituting for La, ($La_{0.7}Ce_{0.3}B_6$ (100), $La_{0.82}Pr_{0.18}B_6$ (100), $La_{0.85}Nd_{0.15}B_6$ (100), $La_{0.82}Pr_{0.18}B_6$ (110)) [92O1]. Crystal diameter: 0.5 cm.

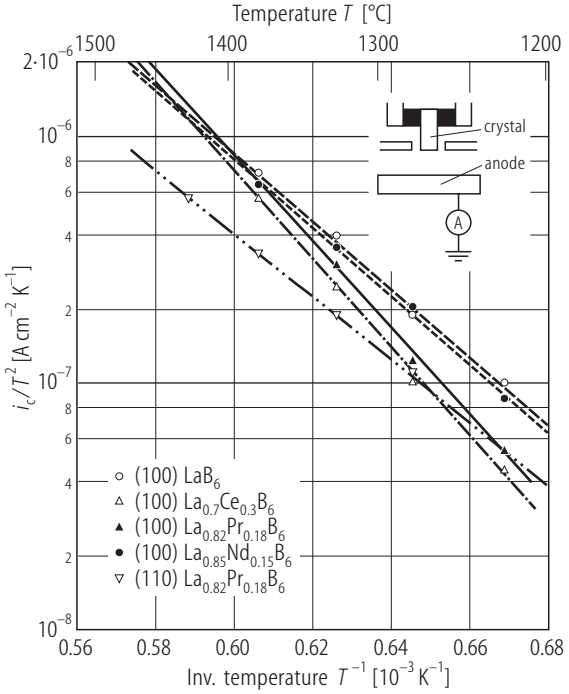

Fig. 6

LaB_6 (:Ce, Pr, Nd). Relationship between brightness and total emission current (samples like in Fig. 5) [92O1]. Acceleration voltage: 20 kV, cathode temperature 1550 °C, vacuum $1 \cdot 10^{-6}$ Torr.

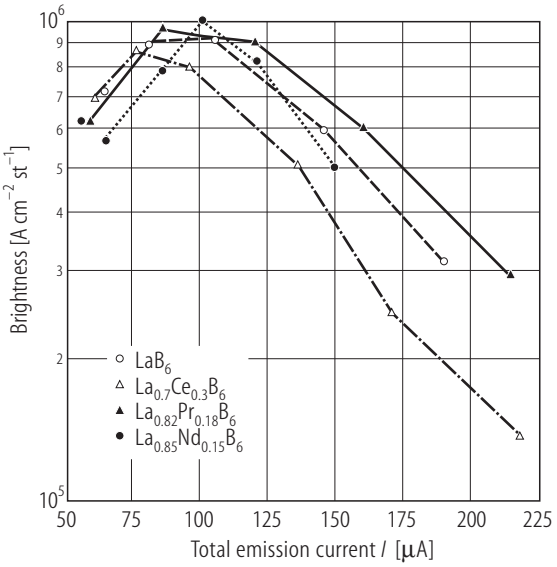

Fig. 7.

LaB_6, CeB_6. Richardson plots for LaB_6 and CeB_6 crystals with excess B compared with pure material [96O1]. Crystal diameter: 0.5 cm.

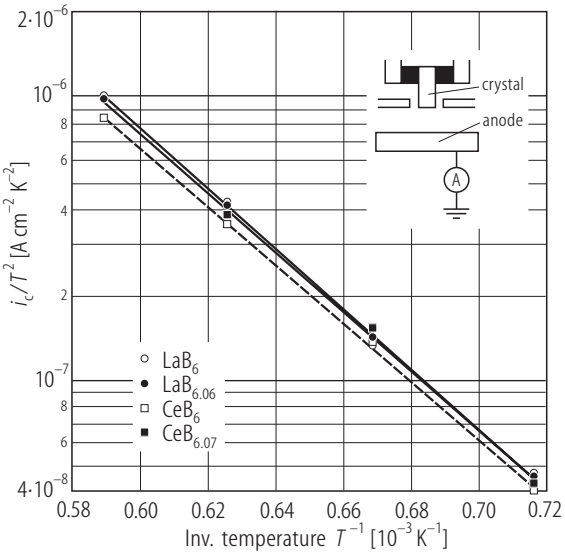

Fig. 8.

LaB_6. Calculated electron density distribution [75P1]. For transition energies see table.

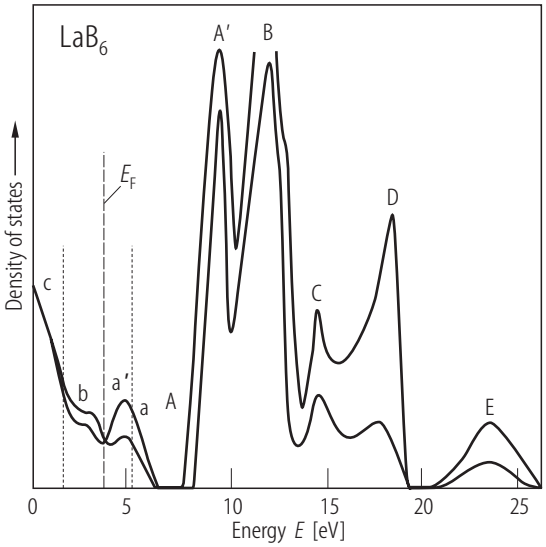

Fig. 9.

LaB_6.**(a)** Energy dependent spectra of electrons emitted from the E_0 = 50 eV He^+ ions interacting with the LaB_6 (001) surface; incidence angles 10, 20, 30°, fixed scattering angle of 90°. **(b)** Energy dependent spectra of electrons ejected from the LaB_6 (001) surface by excitation with He I light (α = 30°, θ = 115°) [96S].

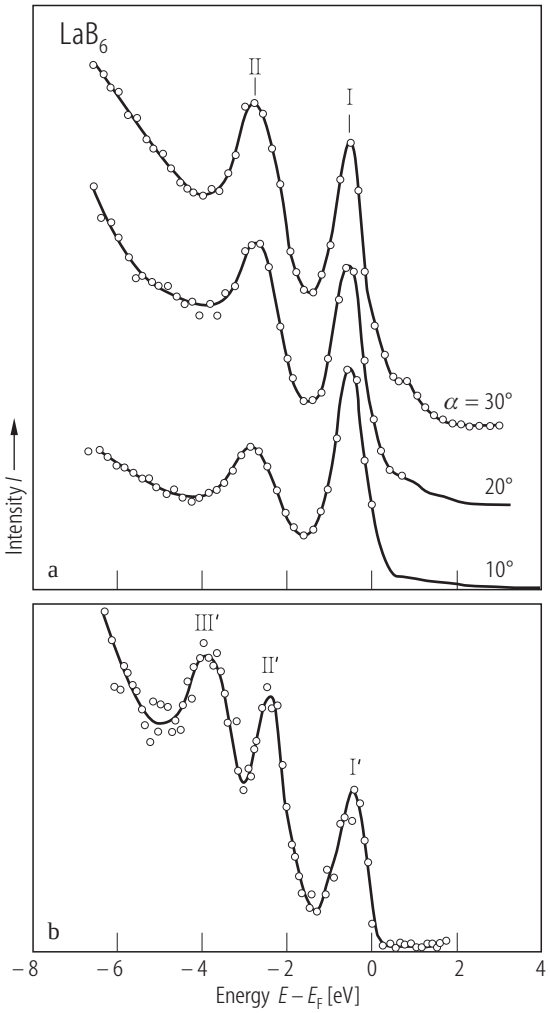

Fig. 10.

LaB_6 (:Ce, Pr, Nd). Variation of the lattice constant by the substitution of Ce, Pr, Nd for La [92O2].

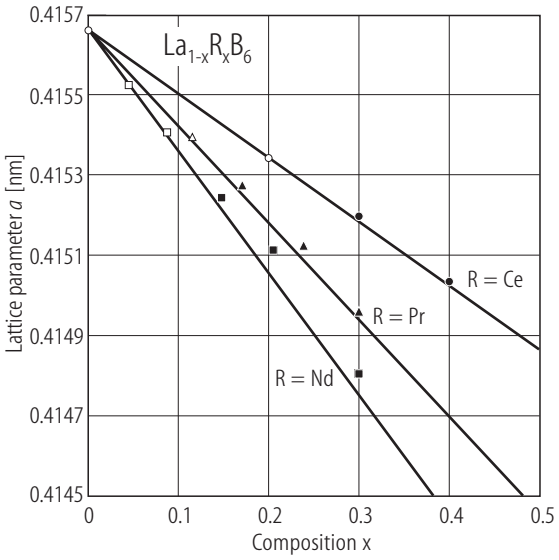

Fig. 11.

LaB_6. Raman spectra of samples synthesized with an excess of boron [93Y].

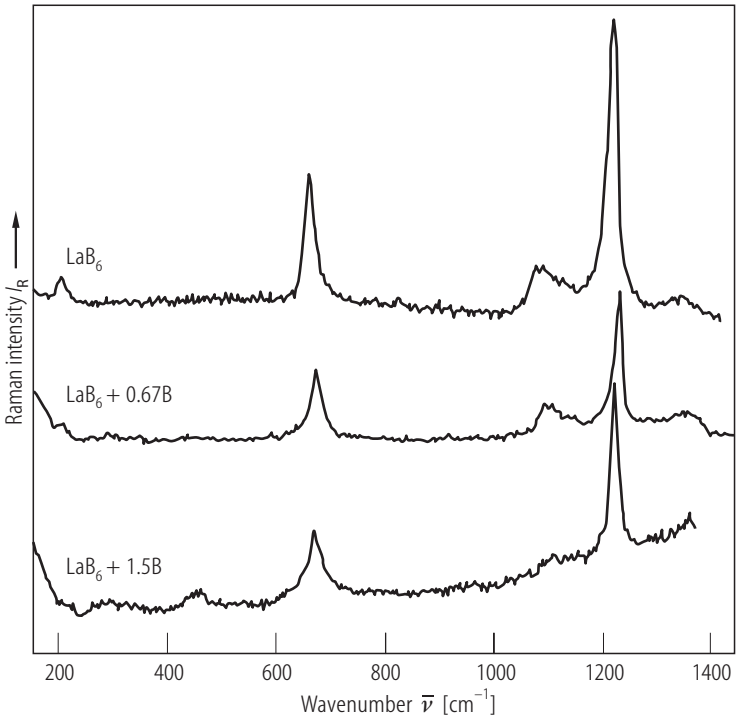

Fig. 12.

LaB_6. Comparison of observed Raman wavenumbers (stoichiometric LaB_6 (circles) and LaB_6 with excess B (crosses)) with the calculated dispersion curves [93Y].

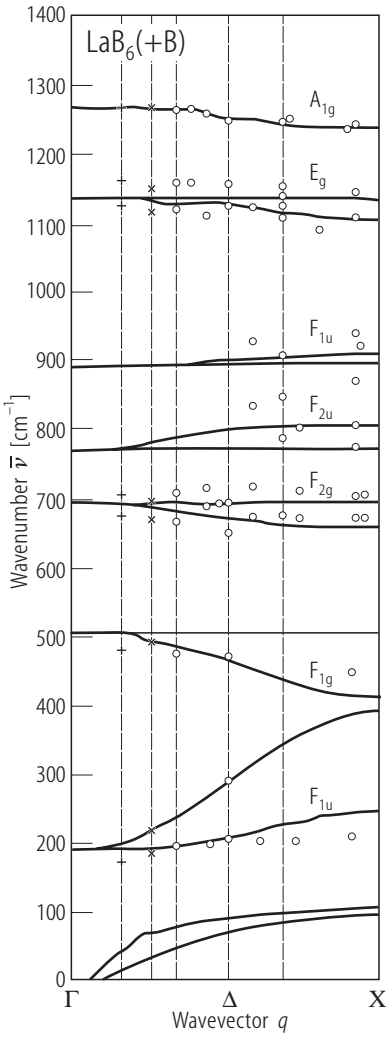

Fig. 13.

Metal hexaborides. Wavenumbers of the phonon symmetry modes A_{1g}, E_g, T_{2g} and T_{1u} vs. lattice parameter for divalent EuB_6, intermediate valent SmB_6 and trivalent YB_6, GdB_6, NdB_6, CeB_6 and LaB_6 [86Z]. Circles, experimental data; solid lines, averaged and extrapolated; dashed lines, assumed variation based on the experimental data for EuB_6.

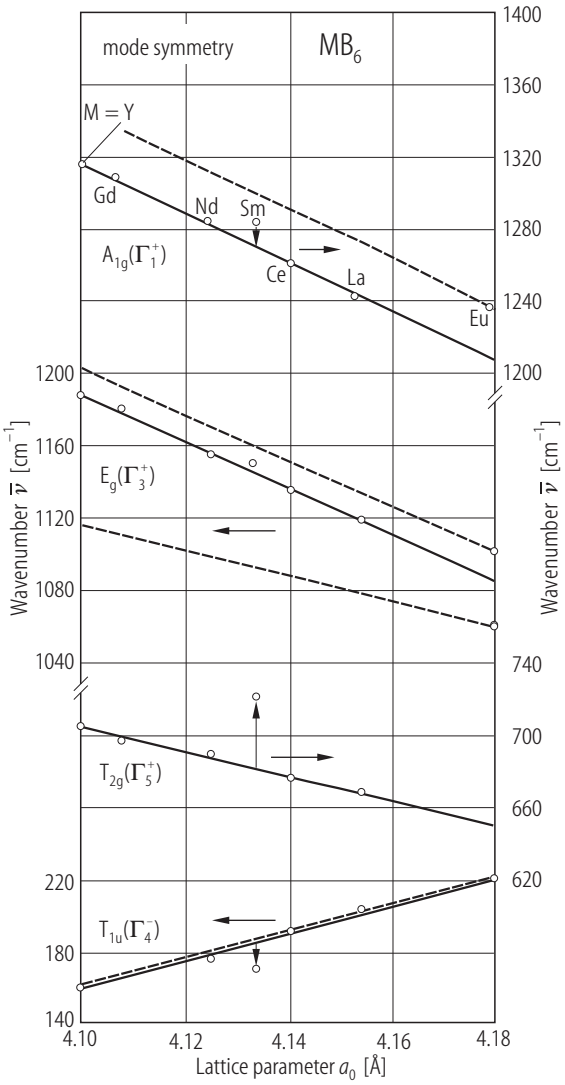

Fig. 14.

Metal hexaborides. Phonon frequencies obtained from the IR absorption spectra (calculated from the measured reflectivity spectra by Kramers-Kronig transformation). Same symbols are used for phonons in different compounds, which can be probably attributed to one another. The dashed lines represent the Raman frequencies in Fig. 21. The full lines combine the plasmon polariton frequencies of the semiconducting hexaborides EuB_6 and YbB_6, and the arrows indicate the shift to the related resonance frequency in metallic LaB_6 (softening of the high frequency F_{1u} mode and hardening of the low frequency F_{1u} mode) obviously caused by the high carrier concentration [99W].

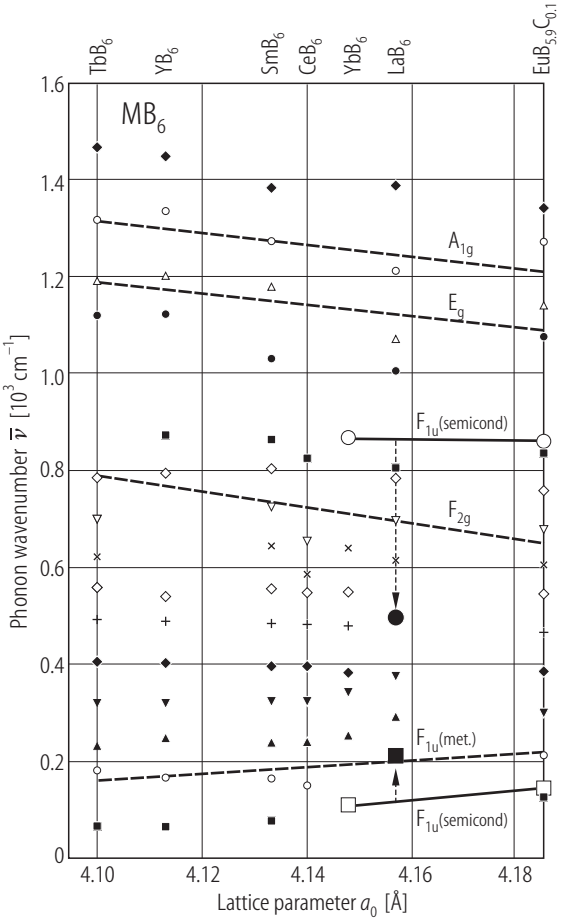

Fig. 15.

LaB_6. Calculated phonon dispersion curves. The dashed lines have been calculated from the observed sound velocities. Frequencies measured by Raman and neutron scattering are shown by open symbols [85T].

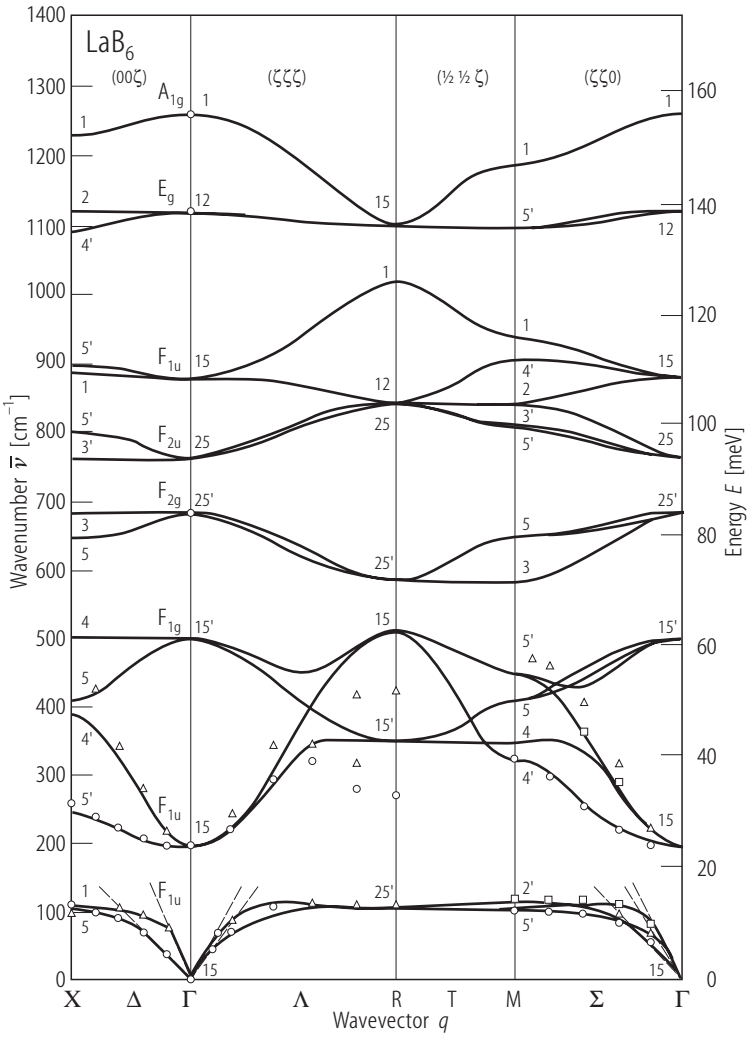

Fig. 16.

LaB_6. Point-contact spectra with the contact axis parallel to [111]. (*1*) spectrum in the thermal regime (contact resistance R = 0.9 Ω, bath temperature T = 4.2 K); (*2*) spectrum in the ballistic regime (R = 3 Ω, T = 1.7 K); (*3*) spectrum in the ballistic regime (R = 2.3Ω, T = 4.2 K); dashed line, background signal; (*4*) calculated double-phonon maximum related to the first peak of spectrum (*3*) [88S].

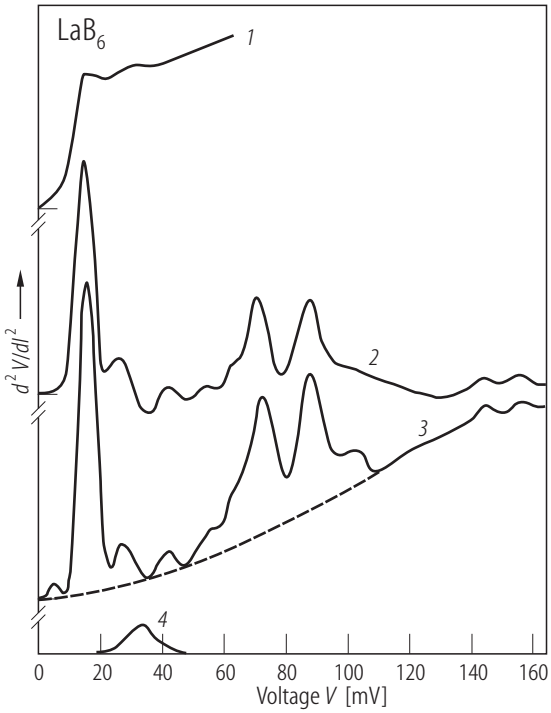

Fig. 17.

$La^{11}B_6$. Phonon dispersion curves for [001], [110] and [111] directions, measured by inelastic neutron scattering [85S]. Dashed straight lines: calculated from elastic properties.

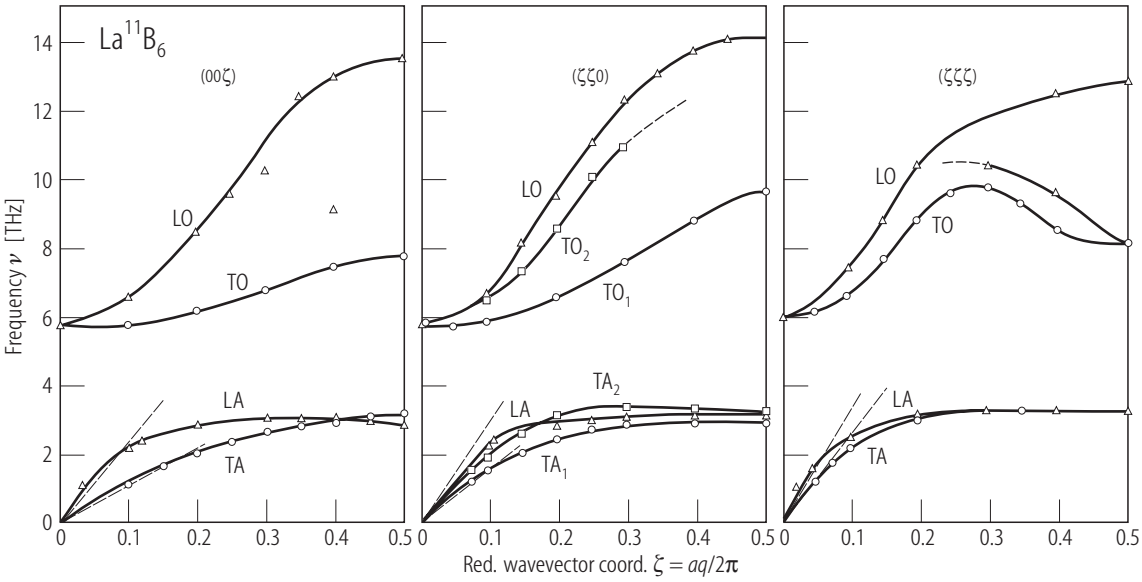

Fig. 18.

LaB_6. Entire phonon spectrum. **(a)** Solid curves, FT Raman spectrum [97S]; dashed curve, point contact spectrum [88S]; **(b)** circles, density of states determined by inelastic neutron scattering [82S], solid line, theoretically calculated density of states [82S], dashed line, theoretically calculated density of states [78G].

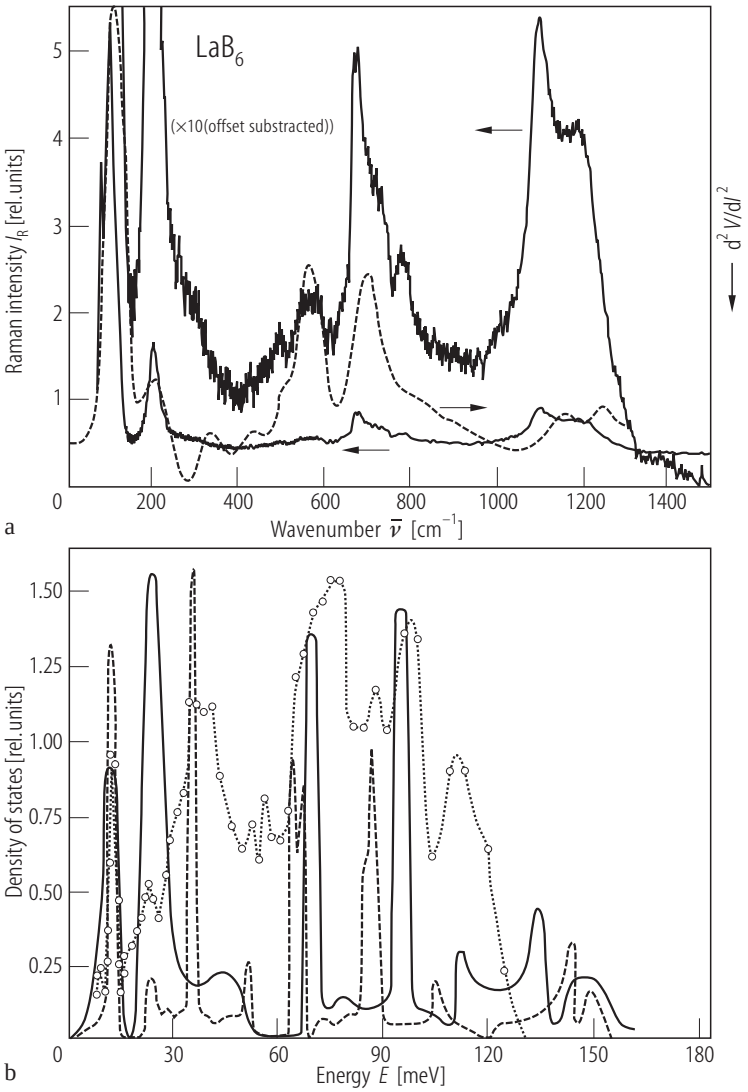

Fig. 19.

LaB_6. Low frequency part of the FT-Raman spectrum [97S] compared with the phonon branches obtained on $La^{11}B_6$ by inelastic neutron scattering [85S] (the results for all the crystallographic directions are collected in the left diagram).

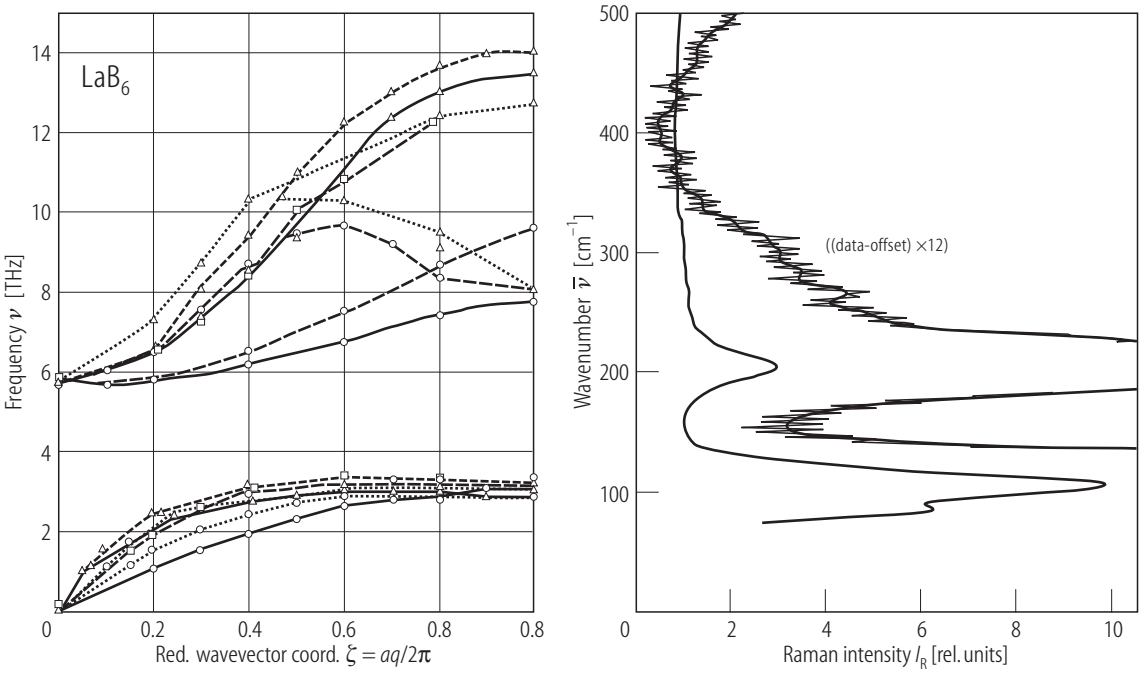

Fig. 20.

LaB_6. Typical high-resolution electron energy loss spectra of pure and oxygen-covered surfaces; **(a)** (100) surface, clean and covered with a two-atomic layer of oxygen, **(b)** (111) surface, clean and covered with a two-atomic layer of oxygen [96Y2].

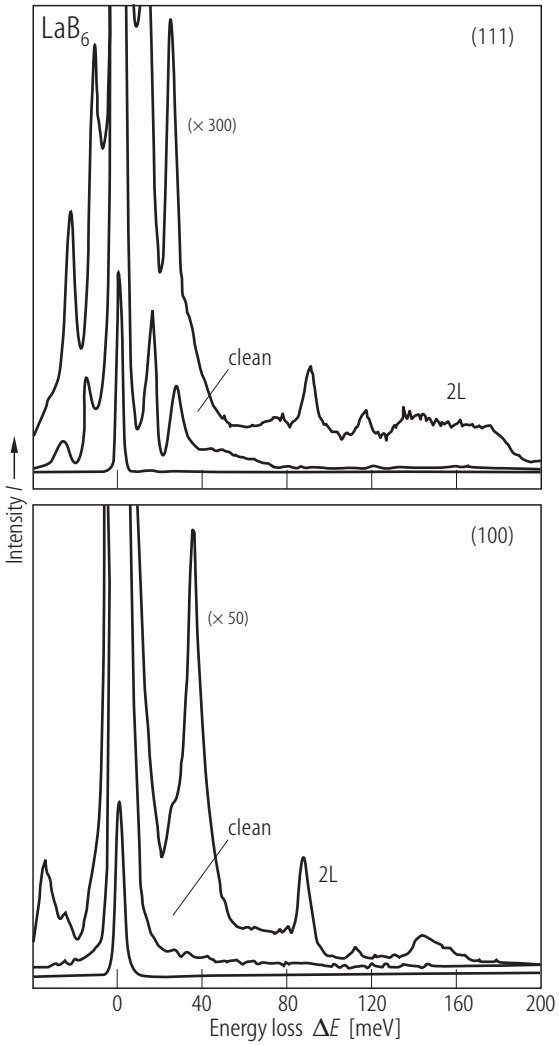

Fig. 21.

Metal hexaborides. IR diffuse reflectance spectra of representative MB_6 compounds with two-valent Ca, Sr and Yb, and three-valent Nd, Gd, La, Tb and Dy metal atoms [88T, 93Y].

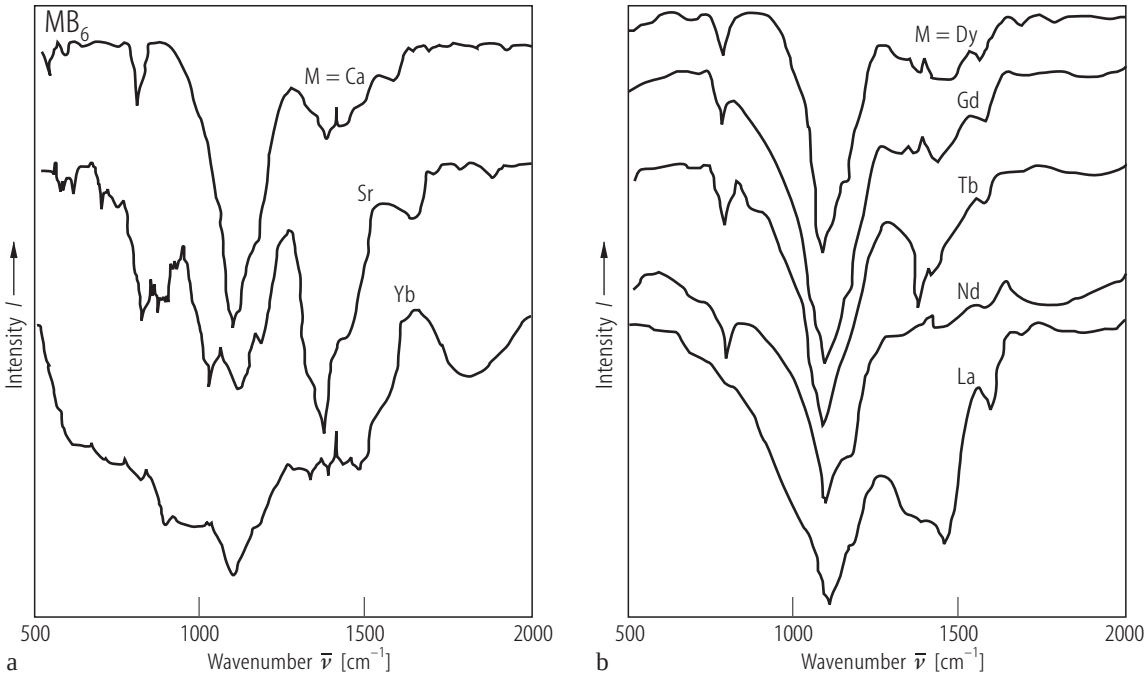

Fig. 22.

Metal hexaborides. Pressure dependence of the electrical resistivity; $\rho(p)/\rho(0)$ vs. hydrostatic pressure p. Full lines, monocrystalline LaB_6, EuB_6 and YbB_6 [91S1], dashed lines, LaB_6, SmB_6 prepared from starting ratios Sm:B 1/7, 1/9, 1/12 (effect increases this way), YbB_6, EuB_6 [81K].

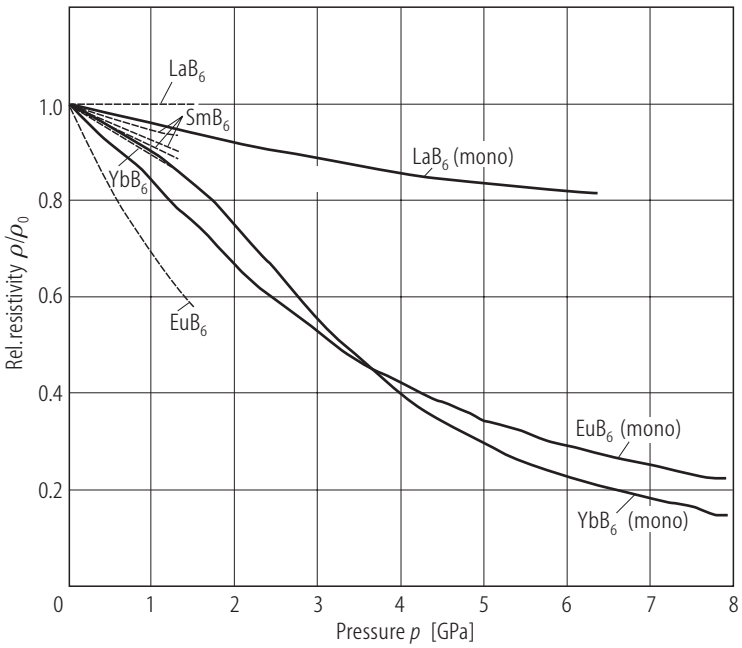

Fig. 23.

Metal hexaborides. Pressure dependence of the thermoelectric power S for LaB_6, YbB_6 and EuB_6 [81K].

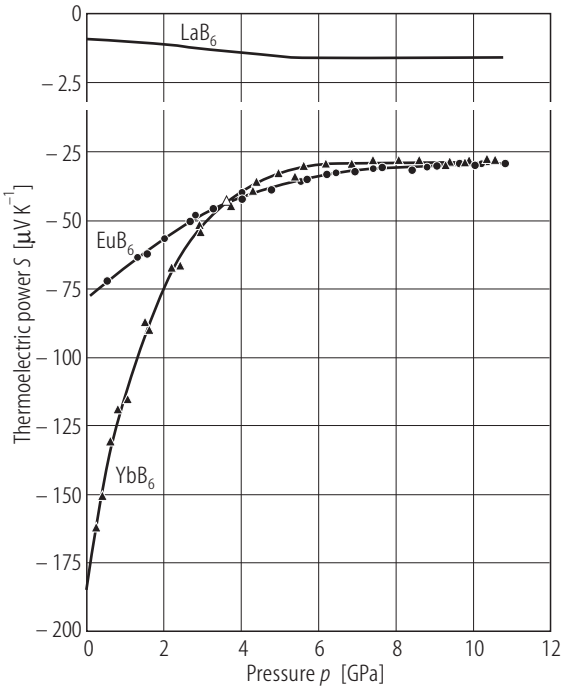

Fig. 24.

LaB_6. Dielectric function vs. photon energy. ε_1, real part, ε_2 imaginary part, $-\mathrm{Im}\ \varepsilon^{-1}$) energy loss function, ε^e contribution of free electrons (determined by making model assumptions for the interband transitions) [81S].

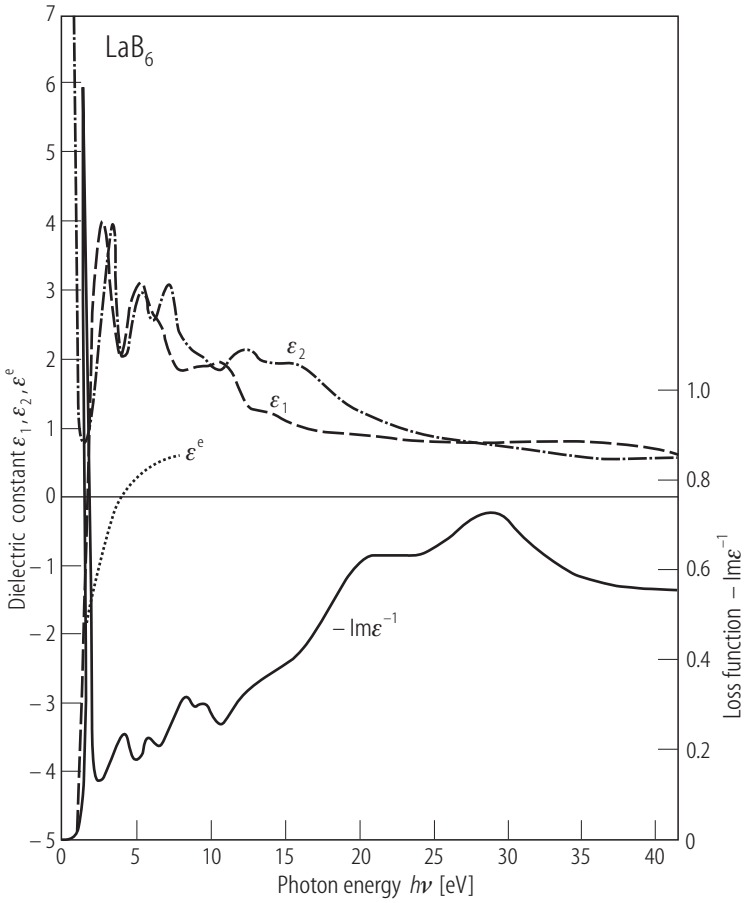

Fig. 25.

LaB_6. Reflectivity vs. wavenumber for samples obtained by different preparation conditions. *(1)* molten, *(2)* film deposited at 200 °C, *(3)* film deposited at 550 °C, *(4)* film deposited at 650 °C [80B].

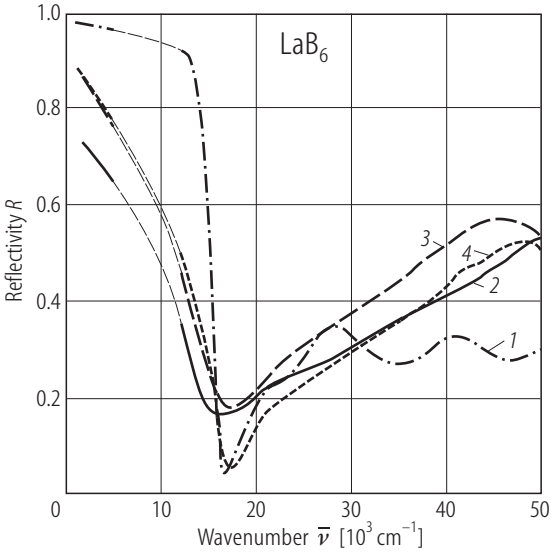

Fig. 26.

Metal hexaborides. Optical reflectivity spectra; R vs. photon energy. Long-dashed curve, LaB_6, solid curve, SmB_6, short-dashed curve, EuB_6 [81S].

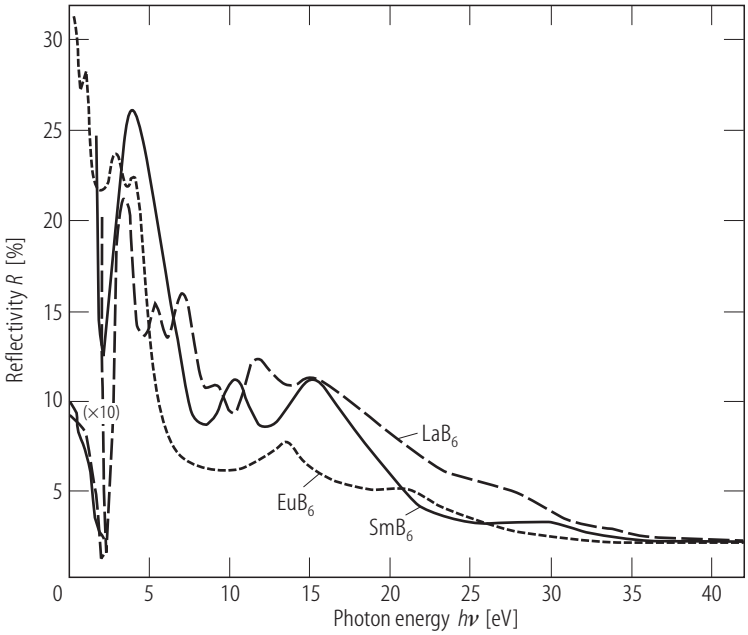

Fig. 27.

Metal hexaborides. Entropy vs. T for LaB_6, ferromagnetic EuB_6, antiferromagnetic EuB_6 [80F].

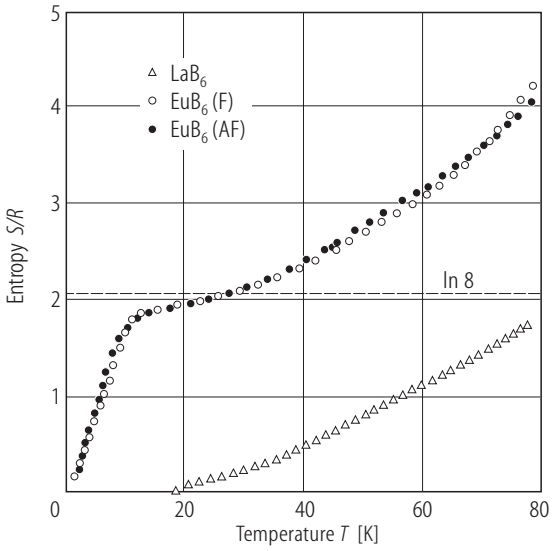

Fig. 28.

LaB_6. Molar specific heat C_p vs. T. Full line, [91P2, 91S1], dashed line [85P], dash-dotted line [85S, 78R]. Insert: Molar specific heat divided by T^3 vs. ln T/T_0. T_0 = 1 K.

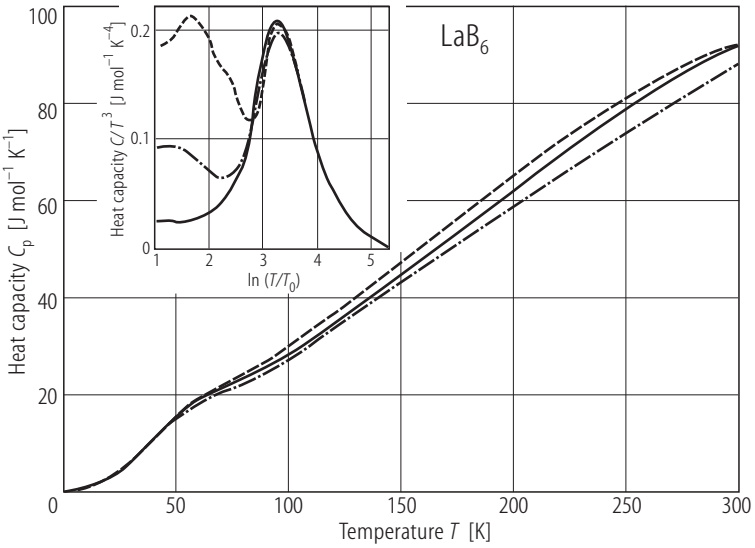

Fig. 29.

LaB_6 :Ce. Hardness vs. T and vs. homologous T (= T/T_m with T_m, melting point) [94O1].

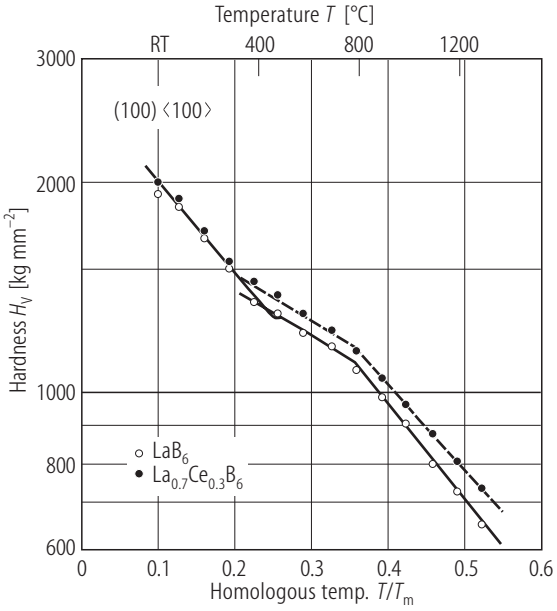

Fig. 30

LaB_6, CeB_6 :B. Evaporation rate of pure LaB_6 and CeB_6 with excess B compared with the corresponding pure crystals [96O1].

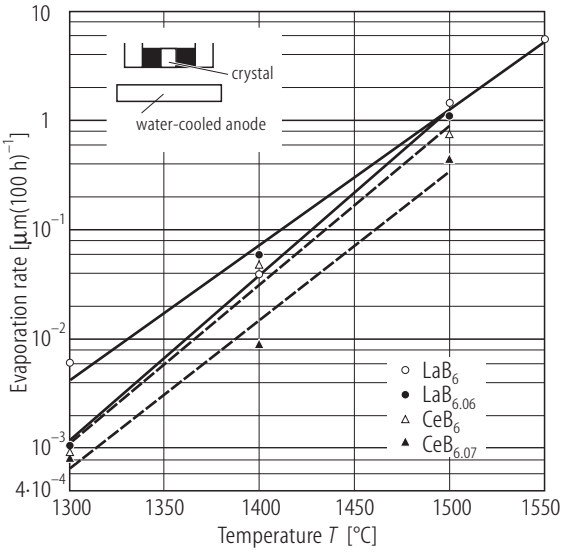

Fig. 31.

Metal hexaborides. Characteristic Einstein temperatures of the Ln atoms vs. atomic number of the Ln element; full circles [94K]; triangles [99T].